

Combination of serum FOXR2 and transvaginal three-dimensional power Doppler ultrasonography in the diagnosis of uterine lesions

Ping Zhang^{A,D,F}, Qiong Zhou^{B,C}, Zhiyong Zeng^{E,F}

Department of Ultrasound, Hunan Provincial People's Hospital (The First Hospital Affiliated with Hunan Normal University), Changsha, China

A – research concept and design; B – collection and/or assembly of data; C – data analysis and interpretation;

D – writing the article; E – critical revision of the article; F – final approval of the article

Advances in Clinical and Experimental Medicine, ISSN 1899–5276 (print), ISSN 2451–2680 (online)

Adv Clin Exp Med. 2024;33(7):699–708

Address for correspondence

Zhiyong Zeng

E-mail: zhiyongzeng2022@163.com

Funding sources

None declared

Conflict of interest

None declared

Received on March 1, 2023

Reviewed on June 23, 2023

Accepted on August 18, 2023

Published online on October 13, 2023

Abstract

Background. Cervical carcinoma and endometrial carcinoma are the most common gynecologic cancers worldwide. Forkhead-box R2 (FOXR2) plays an important role in the progression of various malignant tumors. However, the effects of FOXR2 on the development of uterine lesions remain unclear.

Objectives. This prospective observational study aimed to investigate the diagnostic performance of FOXR2 and transvaginal three-dimensional power Doppler ultrasonography (3D-PDU) for malignant uterine lesions.

Materials and methods. This study included 404 uterine lesion patients and 200 healthy individuals who visited the hospital for a physical examination from April 2014 to May 2016. All patients received FOXR2 detection and 3D-PDU examination at admission. The demographic data and clinical data, including age, body mass index (BMI), and the International Federation of Gynecology and Obstetrics (FIGO) stage, were collected. All the patients were followed up for 5 years. The overall survival (OS) was analyzed using Kaplan–Meier (K–M) curve analysis. The diagnostic value of FOXR2 and 3D-PDU was evaluated using receiver operating characteristic (ROC) curves.

Results. Serum levels of FOXR2 mRNA were upregulated in patients with malignant uterine lesions. Patients with high expression of FOXR2 showed a higher expression of the cancer biomarkers CA125, CA199, CEA, and SCCA. It was also found that FOXR2 expression was associated with the clinical outcomes of patients with malignant uterine lesions. Moreover, higher expression of FOXR2 predicted a poor prognosis. The combined use of FOXR2 and 3D-PDU showed favorable potential for the diagnosis of malignant uterine lesions, especially for cervical carcinoma and endometrial carcinoma.

Conclusions. The combination of serum FOXR2 and transvaginal 3D-PDU has a potential in the diagnosis of uterine lesions.

Key words: diagnosis, FOXR2, 3D-PDU, uterine lesions

Cite as

Zhang P, Zhou Q, Zeng Z. Combination of serum FOXR2 and transvaginal three-dimensional power Doppler ultrasonography in the diagnosis of uterine lesions.

Adv Clin Exp Med. 2024;33(7):699–708.

doi:10.17219/acem/171382

DOI

10.17219/acem/171382

Copyright

Copyright by Author(s)

This is an article distributed under the terms of the Creative Commons Attribution 3.0 Unported (CC BY 3.0) (<https://creativecommons.org/licenses/by/3.0/>)

Background

Cervical carcinoma and endometrial carcinoma are the most common gynecologic cancers in developed countries, ranking 2nd and 4th, respectively, in malignant tumors of the female reproductive system.^{1–4} In the last decade, the incidence and mortality rates of malignant gynecologic cancers have been increasing year by year.^{5–7} As reported, the 5-year survival for cervical carcinoma patients with high tumor stage is no more than 60%.⁸ Although huge progress has been made in the treatment, such as radiotherapy and chemotherapy, the long-term survival for patients with tumor metastasis is still not satisfactory.^{9–11} Therefore, finding a novel diagnostic method is important.

Three-dimensional power Doppler ultrasonography (3D-PDU) is a new imaging technique widely used in gynecology, especially in gynecologic oncology.^{12–14} The 3D-PDU exhibits a similar diagnostic performance as magnetic resonance imaging (MRI) in predicting deep myometrial invasion and cervical involvement for endometrial cancer staging.^{15–17} Zhang et al. found that combined applications of 3D-PDU and MRI showed a better effect on the staging diagnosis of endometrial cancer with hepatitis B virus infections than a single examination using 3D-PDU or MRI.¹⁸ Several biomarkers are proven to be associated with the diagnosis of endometrial carcinoma and cervical carcinoma, including CA125, CA15-3, CA19-9, CEA, and SCCA.^{19–21} Among these biomarkers, forkhead-box R2 (FOXR2) is involved in gynecologic oncology. A previous study revealed the upregulation of FOXR2 in the tissues of patients with ovarian cancer, suggesting an obvious association of the biomarker with the prevalence of ovarian cancer.²² Another study demonstrated that FOXR2 accelerated tumor metastasis and the growth of ovarian cancer cells by stimulating angiogenesis and activating the Hedgehog signaling pathway.²³ However, the evidence shows that FOXR2 serves as a tumor promoter in different cancers, such as human colorectal cancer,²⁴ lung cancer²⁵ and thyroid cancer.²⁶ The clinical significance of FOXR2 in uterine lesions needs further investigation.

Objectives

We conducted an observational study to investigate the association between the expression of FOXR2 and the prognosis of uterine lesion patients, and analyze the diagnostic performance of combined applications of FOXR2 and 3D-PDU for uterine lesions.

Materials and methods

Participants and samples

Our prospective observational study included 404 uterine lesion patients who reported to Hunan Provincial People's Hospital (The First Hospital Affiliated with Hunan Normal University), Changsha, China, for treatment between April 2014 and May 2016. All patients were diagnosed with uterine lesions through histological analysis. The inclusion criteria were as follows: 1) no history of severe drug allergy; 2) no serious cardiovascular diseases, including uncontrolled hypertension, coronary heart disease, angina pectoris, heart failure, or myocardial infarction; and 3) patients without dyspnea or severe pulmonary insufficiency. The following patients were excluded: 1) patients who received chemotherapy or radiotherapy before the study; 2) patients who underwent a traumatic operation before examination, such as hysteroscopy and diagnostic curettage; and 3) patients with other cancers. The tumor stage was evaluated according to the International Federation of Gynecology and Obstetrics (FIGO) criteria.²⁷ Additional 200 healthy female patients who visited the hospital for physical examinations during the same period were enrolled in our study as controls. Blood samples were collected from all participants. The tumor tissues of all patients were obtained and immediately stored at –80°C for the following analysis. Fasting peripheral venous blood samples (5 mL) were collected from all patients within 24 h of admission and stored at –80°C for the following experiments. This study obtained the approval from the Ethics Committee of the Hunan Provincial People's Hospital (The First Hospital Affiliated with Hunan Normal University, approval No. HuNPPH-20150058). Written informed consent was provided by all participants. The study conformed to the principles outlined in the Declaration of Helsinki.

Calculation of sample size

The following formulas (Equation 1,2) were implemented:

$$N_{\text{SEN}} = \frac{Z_{1-\alpha/2}^2 \text{SEN}(1 - \text{SEN})}{d_{\text{SEN}}^2 P} \quad (1)$$

$$N_{\text{SPE}} = \frac{Z_{1-\alpha/2}^2 \text{SPE}(1 - \text{SPE})}{d_{\text{SPE}}^2 P} \quad (2)$$

Minimal sample size (N) = max (N_{SEN} , N_{SPE}), where α stands for the test level, d indicates the tolerance error, Z represents the Z score, $Z_{1-\alpha/2}$ indicates that the sample follows a standard normal distribution, $Z_{1-\alpha/2}$ is identified as 1.96, SEN stands for sensitivity, SPE indicates specificity, and P represents the prevalence of disease.

The mean SEN value was 0.828 and the SPE level was 0.834, according to previous studies. The p-value was 0.456 for the prevalence of malignant uterine lesions, and 0.544 for the prevalence of benign lesions. Thus, $\alpha = 0.05$, $Z_{1-\alpha/2} = 1.96$, $d = 0.1$, $N_{SEN} = 120$, $N_{SPE} = 98$, and minimal sample size (N) = 120.

Reverse transcription-quantitative polymerase chain reaction

Total RNAs were extracted from serum samples using Trizol reagent (Tiangen Biotech, Beijing, China). The RNA concentrations were detected using a NanoDrop spectrophotometer (Thermo Fisher Scientific, Waltham, USA). Subsequently, reverse transcription of RNA was conducted using a PrimeScript RT reagent Kit (Takara, Shiga, Japan), and the target genes were quantified using ABI PRISM7300 Sequence Detection System (Applied Biosystems, Waltham, USA) with the SYBR Premix ExTaq (Thermo Fisher Scientific). The following primers were used: F 5'-ACTGGGTCTCATGATGGTGG-3' and R 5'-CTCCATCCAGGAGGTGATCT-3' for FOXR2 and F 5'-TAGACTTTCGAGCAGGAGATG-3' and R 5'-ACTCATCGTACTCCTGCTTG-3' for β -actin. The β -actin was utilized as an internal control, and the relative expression of FOXR2 mRNA was calculated using the $2^{-\Delta\Delta C_t}$ method.

Transvaginal three-dimensional power Doppler ultrasonography (3D-PDU)

The vaginal volume probe with the power Doppler mode (Voluson E8; GE Healthcare, Chicago, USA) was used to examine the uteri of all patients. The sampling volume was placed on the color central blood flow, adjusted to about 5 mm from the edge of the tumor. Subsequently, the piezoelectric chip of the probe was rotated automatically at a 90° angle to scan the whole lesion. A complete three-dimensional power Doppler image was obtained. The thickness, shape, echo, and integrity of the endometrial contour, the location, number, size, shape, boundary, echo, and surface of lesions, as well as the relationship between basement and endometrium, were evaluated. The Virtual Organ Computer-aided Analysis (VOCAL) software (GE Healthcare) for the 3D power Doppler histogram analysis with computer algorithms was used to analyze the indices of blood flow and vascularization, including the vascularization index (VI), flow index (FI) and vascularization flow index (VFI).

Data collection and follow-up

Demographic data of all patients, including age, body mass index (BMI) and tumor stage, were collected. Serum levels of cancer-related biomarkers, including serum CA15-3, CA125, CA19-9, CEA, and SCCA, were

determined using chemiluminescence immunoassay, as reported in a previous study.²⁸ All patients were followed up for 5 years from admission to death or the last follow-up.

Statistical analyses

First, the Kolmogorov–Smirnov analysis was used to confirm whether the data were normally distributed. The normally distributed data were expressed as mean \pm standard deviation ($M \pm SD$), and non-normally distributed data were presented as median with range. The heterogeneity of variance was analyzed using Levene's test. For normally distributed data (data expressed as $M \pm SD$), the comparison between 2 groups was conducted using Student's t-test, while the non-normally distributed data (data expressed as median with range) were compared using the Mann–Whitney U test. The rates were compared with the χ^2 test. A receiver operating characteristic (ROC) curve was used to analyze the diagnostic value. A Kaplan–Meier (K–M) curve with a log-rank test were used to examine the survival time. A p-value < 0.05 was considered statistically significant. All calculations were made using SPSS 18.0 (SPSS Inc., Chicago, USA) and GraphPad v. 6.0 (GraphPad Software, San Diego, USA) software.

Results

Basic clinical characteristics of all patients

This prospective observational study included 204 cases of malignant uterine lesions, 200 cases of benign lesions and 200 healthy controls. All participants were consecutively enrolled. Compared to the benign lesion group, the malignant lesion group had higher serum levels of CA15-3, CA125, CA19-9, CEA, and SCCA, and a higher ratio of positive human papillomavirus (HPV). No significant difference was found for age and BMI between the malignant lesion group and the benign lesion group, as well as between the uterine lesion group and the healthy group (Table 1).

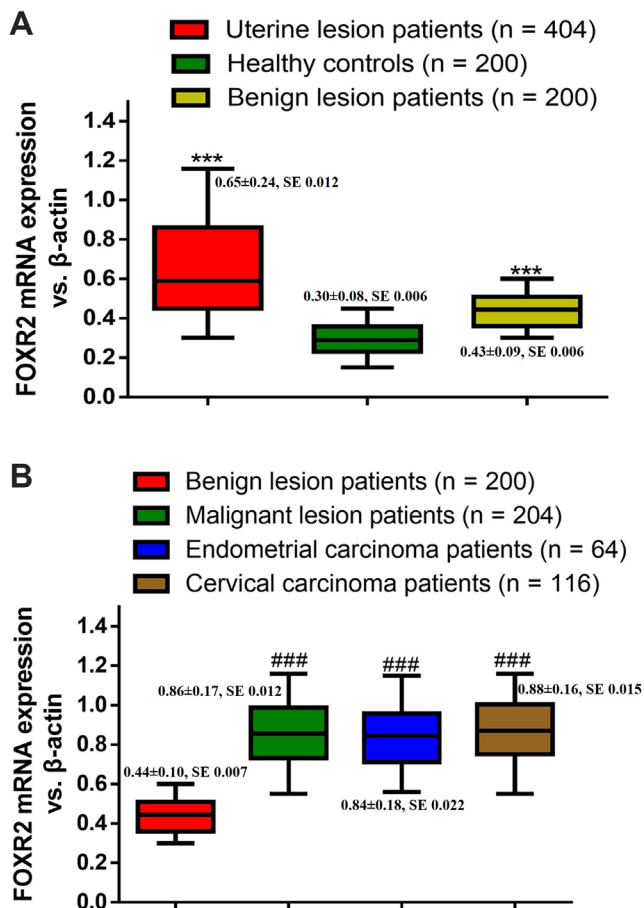
Serum levels of FOXR2 were elevated in malignant uterine lesion patients

Subsequently, the expression of FOXR2 in serum samples and tissue samples was determined. As shown in Fig. 1A, the serum FOXR2 expression was notably upregulated in all uterine lesion patients, including benign lesion patients, compared to healthy controls ($p < 0.001$). The FOXR2 expression in tissue samples was increased in all malignant uterine lesion patients, endometrial carcinoma patients and cervical carcinoma patients compared to benign uterine lesion patients (Fig. 1B, $p < 0.001$). These findings illustrate that FOXR2 expression is upregulated in patients with malignant uterine lesions.

Table 1. Basic clinical characteristics of all patients

Variables	All patients (n = 404)	Malignant lesions (n = 204)	Benign lesions (n = 200)	Healthy (n = 200)	Test value (t, U or χ^2)	p-value*
Age [years] ^a	53.46 \pm 5.05	53.38 \pm 5.24	53.55 \pm 4.85	53.10 \pm 4.63	-0.343	0.732
BMI [kg/m ²] ^a	21.20 \pm 5.00	21.05 \pm 4.85	21.34 \pm 5.17	21.31 \pm 5.28	-0.608	0.544
CA153 [U/mL] ^b	39.91 (32.25, 49.32)	49.13 (45.62, 54.77)	32.21 (30.37, 34.28)	22.09 (20.82, 23.49)	41	<0.001
CA125 [U/mL] ^b	50.85 (30.53, 68.30)	68.26 (59.76, 77.53)	30.38 (25.27, 35.88)	22.69 (19.16, 27.14)	0	<0.001
CEA [ng/mL] ^b	7.46 (5.06, 11.96)	11.81 (9.89, 15.39)	5.05 (4.74, 5.29)	2.49 (2.34, 2.64)	0	<0.001
CA199 [U/mL] ^b	47.79 (39.70, 69.88)	69.61 (59.94, 78.78)	39.69 (37.54, 41.92)	17.44 (13.60, 21.15)	66	<0.001
SCCA [μ g/L] ^b	1.51 (1.28, 3.06)	3.04 (1.62, 4.32)	1.31 (1.18, 1.46)	1.02 (0.89, 1.13)	3292	<0.001
Positive HPV, n (%) ^c	147 (36.39)	120 (58.82)	27 (13.50)	14 (7.00)	44.487	<0.001

* comparison for all variables was conducted between the malignant lesion and benign lesion groups; ^a comparison for normally distributed data (data expressed as mean \pm standard deviation (M \pm SD)) was conducted using Student's t-test; ^b non-normally distributed data (data expressed as median with range) were compared using the Mann-Whitney U test; ^c χ^2 test was used for the comparison of rates. Positive human papillomavirus (HPV): at least 1 HPV subtype was positive.



Serum FOXR2 was associated with cancer-related biomarkers and clinical outcomes of malignant uterine lesion patients

To further investigate the role of FOXR2 in uterine lesions, all malignant uterine lesion patients were divided into 2 groups, namely a high FOXR2 expression group and a low FOXR2 expression group, according to the median value of FOXR2 mRNA (0.855 compared to β -actin). Basic characteristics, including levels of tumor markers and the rate

of positive HPV, were detected. As shown in Table 2, serum levels of CA15-3, CA125, CA19-9, CEA, and SCCA were significantly higher in the high FOXR2 group than in the low FOXR2 group for all malignant lesion patients and cervical carcinoma patients (all $p < 0.001$). However, endometrial carcinoma patients with high/low FOXR2 expression showed no significant difference in SCCA expression. Additionally, the ratio of positive HPV ($p < 0.001$ for all comparisons), advanced FIGO stage ($p < 0.001$ for malignant lesions and cervical carcinoma, $\chi^2 = 11.746$ and $p = 0.001$ for endometrial carcinoma), lymph node metastasis (LNM) ($p < 0.001$ for malignant lesions and cervical carcinoma, $\chi^2 = 8.749$ and $p = 0.003$ for endometrial carcinoma), and distant metastasis ($p < 0.001$ for malignant lesions and cervical carcinoma, $\chi^2 = 8.749$ and $p = 0.003$ for endometrial carcinoma) were notably higher in patients with high expression of FOXR2. We further identified the early diagnostic value of FOXR2 for malignant lesions. As shown in Table 3, the ratio of patients with high FOXR2 expression increased along with the FIGO stage in all malignant lesion patients. The K-M curve analysis showed that patients with

***p < 0.001 compared to healthy controls; ###p < 0.001 compared to benign lesion patients; SE – standard error; 95% CI – 95% confidence interval.

of positive HPV, were detected. As shown in Table 2, serum levels of CA15-3, CA125, CA19-9, CEA, and SCCA were significantly higher in the high FOXR2 group than in the low FOXR2 group for all malignant lesion patients and cervical carcinoma patients (all $p < 0.001$). However, endometrial carcinoma patients with high/low FOXR2 expression showed no significant difference in SCCA expression. Additionally, the ratio of positive HPV ($p < 0.001$ for all comparisons), advanced FIGO stage ($p < 0.001$ for malignant lesions and cervical carcinoma, $\chi^2 = 11.746$ and $p = 0.001$ for endometrial carcinoma), lymph node metastasis (LNM) ($p < 0.001$ for malignant lesions and cervical carcinoma, $\chi^2 = 8.749$ and $p = 0.003$ for endometrial carcinoma), and distant metastasis ($p < 0.001$ for malignant lesions and cervical carcinoma, $\chi^2 = 8.749$ and $p = 0.003$ for endometrial carcinoma) were notably higher in patients with high expression of FOXR2. We further identified the early diagnostic value of FOXR2 for malignant lesions. As shown in Table 3, the ratio of patients with high FOXR2 expression increased along with the FIGO stage in all malignant lesion patients. The K-M curve analysis showed that patients with

Table 2. Basic characteristics of all uterine lesion patients

Variables	Malignant lesions (n = 204)				Endometrial carcinoma (n = 64)				Cervical carcinoma (n = 116)			
	high FOXR2 (n = 102)	low FOXR2 (n = 102)	t, U or χ^2	p-value	high FOXR2 (n = 31)	low FOXR2 (n = 33)	t, U or χ^2	p-value	high FOXR2 (n = 63)	low FOXR2 (n = 53)	t, U or χ^2	p-value*
Age [years] ^a	53.26 ± 5.00	53.50 ± 5.50	−0.330	0.741	52.96 ± 5.03	53.26 ± 5.22	−0.233	0.817	52.96 ± 4.85	54.00 ± 5.90	−1.042	0.300
BMI [kg/m ²] ^a	20.94 ± 5.30	21.16 ± 4.38	−0.323	0.747	20.66 ± 6.21	21.26 ± 4.32	−0.448	0.656	20.91 ± 5.07	21.20 ± 4.58	−0.323	0.747
CA153 [U/mL] ^b	54.71 (50.80, 58.74)	46.19 (43.84, 48.46)	1019	<0.001	53.90 (49.37, 58.84)	48.97 (46.28, 53.52)	217	<0.001	54.68 (51.27, 58.33)	46.69 (43.88, 48.42)	264	<0.001
CA125 [U/mL] ^b	76.02 (68.14, 83.34)	59.79 (56.44, 68.52)	1345	<0.001	76.11 (71.50, 84.90)	73.50 (66.03, 79.30)	293	<0.001	77.54 (70.23, 83.64)	59.39 (55.66, 65.44)	197	<0.001
CEA [ng/mL] ^b	15.39 (13.82, 16.94)	9.96 (9.26, 10.87)	168	<0.001	14.40 (13.60, 15.92)	10.41 (9.91, 14.11)	20	<0.001	15.40 (13.80, 17.09)	9.81 (8.94, 11.06)	46	<0.001
CA199 [U/mL] ^b	78.69 (73.96, 82.70)	59.94 (55.96, 64.56)	322	<0.001	77.95 (74.73, 82.26)	60.66 (58.33, 63.08)	8	<0.001	78.89 (74.81, 84.37)	62.21 (55.93, 67.60)	165	<0.001
SCCA [μg/L] ^b	4.03 (1.63, 5.21)	2.60 (1.58, 3.25)	3142	<0.001	1.50 (1.39, 1.61)	1.51 (1.42, 1.61)	481	0.682	5.01 (4.26, 5.48)	3.12 (2.57, 3.55)	200	<0.001
Positive HPV, n (%) ^c	89 (87.25)	31 (30.39)	66.924	<0.001	24 (77.42)	11 (27.27)	50.411	<0.001	59 (93.65)	17 (32.08)	81.193	<0.001
FIGO stage ≥III, n (%) ^c	49 (48.04)	19 (18.63)	19.461	<0.001	10 (32.26)	4 (12.12)	11.746	0.001	33 (52.38)	12 (22.64)	18.871	<0.001
LNM, n (%) ^c	43 (42.16)	17 (16.67)	15.647	<0.001	9 (29.03)	4 (12.12)	8.749	0.003	30 (47.62)	10 (18.87)	18.622	<0.001
Distant metastasis, n (%) ^c	38 (37.25)	15 (14.71)	13.047	<0.001	9 (29.03)	4 (12.12)	8.749	0.003	27 (42.85)	9 (16.98)	15.961	<0.001
Mortality, n (%) ^c	50 (49.02)	17 (16.67)	23.723	<0.001	11 (35.48)	3 (9.09)	20.106	<0.001	35 (55.56)	12 (22.64)	22.756	<0.001

FOXR2 – forkhead-box R2; FIGO – the International Federation of Gynecology and Obstetrics; LNM – lymph node metastasis; *comparison for all variables was made between the high/low FOXR2 expression groups; ^a comparison for normally distributed data (data expressed as mean ± standard deviation (M ± SD)) was conducted using Student's t-test; ^b non-normally distributed data (data expressed as median with range) were compared using the Mann–Whitney U test; ^c χ^2 test was used for the comparison of rates. Positive human papillomavirus (HPV): at least 1 HPV subtype was positive.

Table 3. Forkhead-box R2 (FOXR2) expression in all uterine lesion patients with different International Federation of Gynecology and Obstetrics (FIGO) stages

Indices		FIGO stage			
		I (n = 68)	II (n = 68)	III (n = 36)	IV (n = 32)
Malignant lesions	high FOXR2	20 (29.41)	33 (48.53)	24 (69.44)	25 (78.13)
	low FOXR2	48 (70.59)	35 (51.47)	12 (33.33)	7 (21.87)
Endometrial carcinoma	high FOXR2	9 (13.24)	12 (17.65)	4 (11.11)	6 (18.75)
	low FOXR2	18 (26.47)	11 (16.18)	3 (8.33)	1 (3.13)
Cervical carcinoma	high FOXR2	12 (17.65)	18 (26.47)	18 (50.00)	15 (46.88)
	low FOXR2	27 (39.71)	14 (20.59)	8 (22.22)	4 (12.50)

high FOXR2 had a shorter 5-year survival time compared to those with low FOXR2 in all malignant lesion patients (Fig. 2A, $p < 0.001$), endometrial carcinoma patients (Fig. 2B, $\chi^2 = 6.235$ and $p = 0.0125$) and cervical carcinoma patients (Fig. 2C, $p < 0.001$). These findings suggested that higher FOXR2 expression predicted poor clinical outcomes and prognosis for patients with malignant lesions.

Diagnostic value of serum FOXR2 in benign/malignant uterine lesions

Next, a ROC curve analysis was performed to analyze the diagnostic value of FOXR2 in malignant uterine lesions. The cutoff value of FOXR2 mRNA for malignant uterine lesions was 0.545 compared to β -actin, with

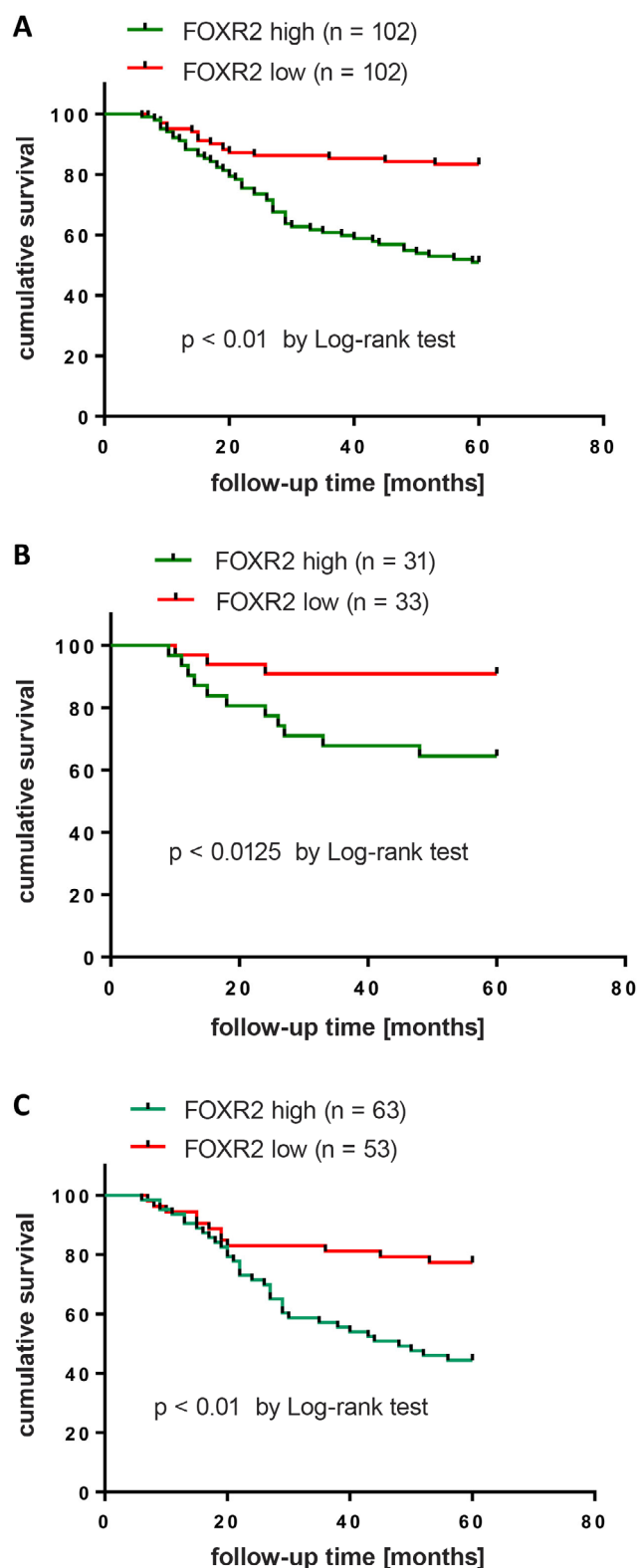


Fig. 2. Kaplan–Meier (K–M) curves of 5-year survival time for malignant lesion patients with high/low expression of forkhead-box R2 (FOXR2). A. K–M curves with log-rank test for all malignant lesion patients; B. K–M curves with log-rank test for endometrial carcinoma patients; C. K–M curves with log-rank test for cervical carcinoma patients

an area under the ROC curve (AUC) of 0.996, sensitivity of 100% and specificity of 87.0% ($p < 0.001$, 95% confidence interval (95% CI): 0.992–0.999, Fig. 3A). The cutoff

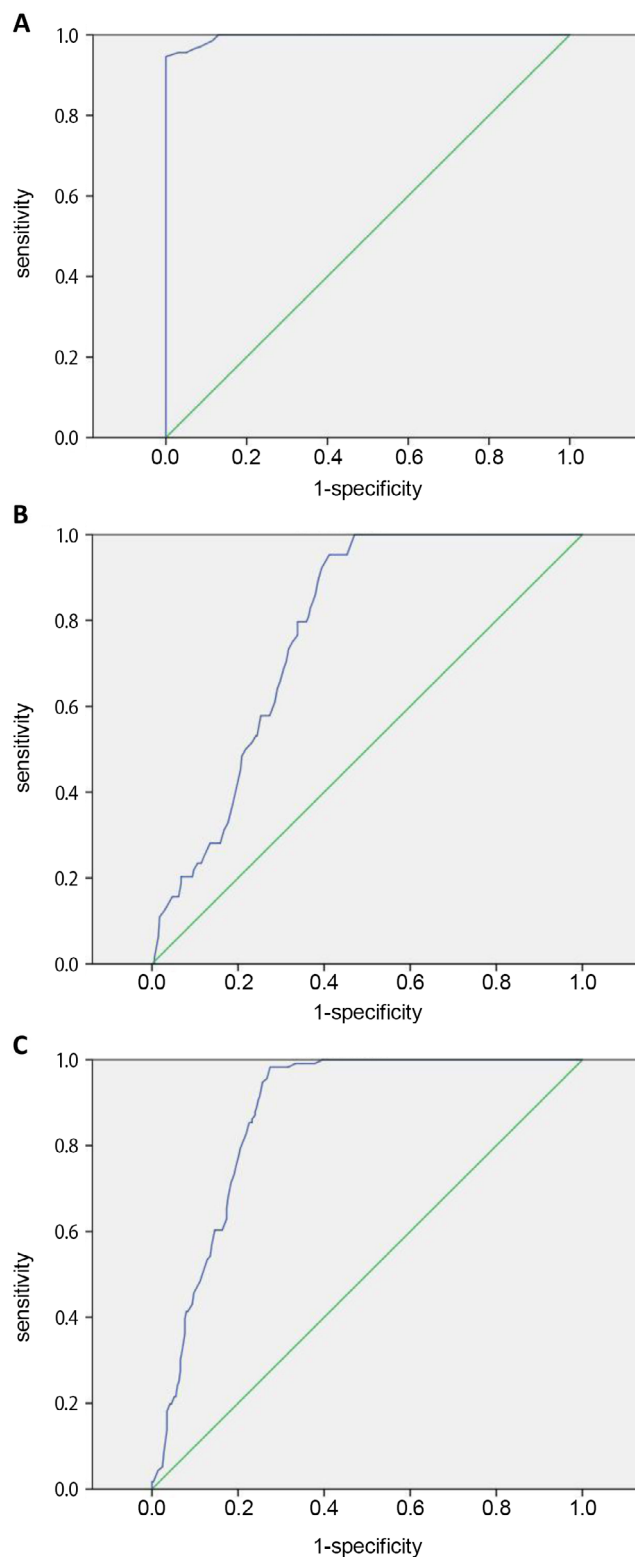


Fig. 3. Receiver operating characteristic (ROC) curves for forkhead-box R2 (FOXR2) levels in the diagnosis of benign uterine lesions and malignant uterine lesions. A. ROC curves for FOXR2 in the diagnosis of benign uterine lesions and malignant uterine lesions; B. ROC curves for FOXR2 in the diagnosis of endometrial carcinoma; C. ROC curves for FOXR2 in the diagnosis of cervical carcinoma

value of FOXR2 for the diagnosis of endometrial carcinoma was 0.645 compared to β -actin, with an AUC of 0.776, sensitivity of 81.3% and specificity of 63.5%

Table 4. Combination of serum forkhead-box R2 (FOXR2) and transvaginal three-dimensional power Doppler ultrasonography (3D-PDU) in the diagnosis of malignant uterine lesions

Indices	Methods	True positive	False positive	True negative	False negative	Sensitivity (%)	Specificity (%)	Accuracy (%)
Malignant uterine lesions	histological	204	0	200	0	100	100	100
	FOXR2	204	26	200	0	100	88.50	93.95
	3D-PDU	201	7	193	3	98.53	96.50	97.52
	FOXR2/3D-PDU	202	5	190	7	96.65	97.44	97.03
Endometrial carcinoma	histological	64	0	340	0	100	100	100
	FOXR2	52	106	234	12	81.25	68.82	70.79
	3D-PDU	62	8	332	2	96.88	97.65	97.52
	FOXR2/3D-PDU	51	6	334	13	79.69	98.24	95.30
Cervical carcinoma	histological	116	0	288	0	100	100	100
	FOXR2	114	79	209	2	98.28	72.56	79.95
	3D-PDU	115	6	282	1	99.14	97.92	98.27
	FOXR2/3D-PDU	110	85	203	5	95.65	70.49	77.67

sensitivity = true positive/(true positive+false negative) × 100%; specificity = true negative/(true negative+false positive) × 100%; accuracy = (true positive+true negative)/(true positive+false negative+false positive+true negative) × 100%.

($p < 0.001$, 95% CI: 0.730–0.823, Fig. 3B). The cutoff value for FOXR2 in the diagnosis of cervical carcinoma was 0.605 compared to β -actin, with an AUC of 0.871, sensitivity of 98.3% and specificity of 75.3% ($p < 0.001$, 95% CI: 0.838–0.905, Fig. 3C). These findings suggested that serum FOXR2 levels might serve as a potential diagnostic marker for malignant uterine lesions. Furthermore, FOXR2 showed satisfactory diagnostic value for endometrial carcinoma and cervical carcinoma.

Combination of serum FOXR2 and transvaginal 3D-PDU in the diagnosis of malignant uterine lesions

Finally, the combined application of serum FOXR2 and transvaginal 3D-PDU in the diagnosis of malignant uterine lesions was analyzed. All patients received a transvaginal 3D-PDU examination at admission. A cutoff value of 0.545 for FOXR2 mRNA was considered diagnostic for malignant uterine lesions, as was a FOXR2 mRNA of 0.645 for endometrial carcinoma and FOXR2 mRNA of 0.605 for cervical carcinoma. As shown in Table 4, the application of FOXR2 combined with 3D-PDU exhibited satisfactory potential in the diagnosis of malignant uterine lesions, with a sensitivity of 96.65%, specificity of 97.44% and accuracy of 97.03%. Moreover, the application of FOXR2 combined with 3D-PDU showed a sensitivity of 79.69%, specificity of 99.17% and accuracy of 98.27% in the diagnosis of endometrial carcinoma, and a sensitivity of 95.65%, specificity of 70.49% and accuracy of 77.67% in the diagnosis of cervical carcinoma. The above results illustrated that FOXR2 combined with transvaginal 3D-PDU might be useful in the diagnosis of malignant uterine lesions, including endometrial carcinoma and cervical carcinoma.

Discussion

Although the diagnostic methods for uterine lesions have developed in the last few decades, the early diagnosis of malignant uterine lesions still requires improvement.^{29–31} Reportedly, the 5-year survival rate for malignant uterine lesion patients with a high tumor stage is no more than 50%.^{32–34} Thus, finding early diagnostic methods and potentially novel biomarkers for malignant lesions of the uterus is of extreme importance. Our study illustrated that FOXR2 was increased in patients with malignant uterine lesions, and a higher FOXR2 expression was associated with a poorer prognosis and shorter 5-year survival time. Moreover, FOXR2, as well as the combined application of FOXR2 and transvaginal 3D-PDU, might be a potential method for the diagnosis of malignant uterine lesions.

Emerging evidence states that FOXR2 is a tumor promoter responsible for the development of different cancers, such as liver cancer,³⁵ lung cancer³⁶ or prostate cancer, among others.³⁷ As reported, FOXR2 was upregulated in breast cancer tissue and was remarkably associated with tumor size and LNM status, indicating that FOXR2 is an independent prognostic factor for breast cancer patients.³⁸ Lu et al. found that FOXR2 promoted proliferation, invasion and epithelial–mesenchymal transition (EMT) of human colorectal cancer cells.²⁴ Nevertheless, limited studies have illustrated the role of FOXR2 in tumors of the female reproductive system. A previous study revealed that FOXR2 expression was elevated in endometrial adenocarcinoma (EAC), and an increased FOXR2 expression was related to a poor prognosis in EAC patients.³⁹ The FOXR2 was also increased in epithelial ovarian adenocarcinoma tissue, and notable correlations between FOXR2 mRNA expression and EMT-related biomarkers were identified in ovarian

adenocarcinoma patients with a high-grade cancer stage.²² In addition, another study found a greater upregulation of FOXR2 in paclitaxel (PTX)-resistant ovarian cancer tissues compared to PTX-sensitive ovarian cancer tissues.⁴⁰ However, the role of FOXR2 has not been well investigated in uterine diseases, especially in endometrial carcinoma and cervical carcinoma. In the present study, we demonstrated that FOXR2 was upregulated in malignant uterine lesion patients and was closely associated with levels of cancer-related biomarkers, namely CA125, CA19-9, CEA, and SCCA. At the same time, the high expression of FOXR2 predicted poorer clinical outcomes and prognosis for patients with malignant uterine lesions.

The most recent study suggests that fluorodeoxyglucose (FDG) positron emission tomography/computed tomography (PET/CT) imaging is recommended for the assessment of various malignancies, such as lung cancer,⁴¹ hypopharyngeal squamous cell carcinoma⁴² and breast cancer.⁴³ The FDG PET/CT also exhibits good diagnostic performance in endometrial carcinoma⁴⁴ and cervical cancer.⁴⁵ Numerous studies report on the application of 3D-PDU in various diseases. Data show that the sensitivity of 3D-PDU is higher than that of digital rectal examination, grey-scale ultrasonography and power Doppler ultrasonography, but its specificity is lower.⁴⁶ The 3D-PDU has been widely used in the diagnosis of benign and malignant uterine lesions. A previous study revealed that 3D-PDU exhibited higher sensitivity and specificity for detecting local recurrence or persistence in cervical carcinoma compared to serum markers (SSCA, CEA and CA125).⁴⁷ Other research suggested that 3D-PDU imaging showed a potential in monitoring early therapeutic responses to concurrent chemo-radiotherapy (CCRT) in patients with cervical cancer.⁴⁸ Belitsos et al. found the indicators of 3D-PDU to be positively correlated with cervical volume except for other pathological characteristics in cervical cancer patients.⁴⁹ Furthermore, compared to early-stage ovarian tumors, the levels of vascular indicators of 3D-PDU were higher in patients with advanced-stage and metastatic ovarian cancers.⁵⁰ The combination of the Mainz ultrasound scoring system with 3D-PDU enhanced its sensitivity and specificity in identifying benign and malignant pelvic tumors.⁵¹ Various biomarkers have been used in the diagnosis of malignant tumors, such as SSCA,⁵² CEA⁵³ and CA125.⁵⁴ However, the combination of biomarkers with 3D-PDU in the diagnosis of malignant uterine lesions was rarely addressed. The present study illustrated that the combination of serum FOXR2 and transvaginal 3D-PDU exhibited a potential in the diagnosis of malignant uterine lesions, especially for endometrial carcinoma and cervical carcinoma.

Limitations

This study has some limitations. First, the samples were collected from a single center. Second, the molecular mechanism of FOXR2 in uterine lesions was not

investigated. Third, the diagnostic value of 3D-PDU was not fully addressed. Further studies are needed to solve the above issues.

Conclusions


In summary, the present study illustrated that serum FOXR2 levels were upregulated in patients with malignant uterine lesions. The FOXR2 was associated with cancer-related biomarkers CA125, CA19-9, CEA, and SCCA. A higher expression of FOXR2 predicted poorer clinical outcomes and shorter 5-year survival times. Both FOXR2 and the combination of FOXR2 with transvaginal 3D-PDU showed potential in the early diagnosis of malignant uterine lesions, especially for endometrial carcinoma and cervical carcinoma. This observational study might provide novel research targets and new diagnostic methods for uterine lesions.


Data availability

All data that support the findings of the study can be obtained from the corresponding author upon reasonable request.

ORCID iDs

Ping Zhang  <https://orcid.org/0009-0000-1000-1822>

Qiong Zhou  <https://orcid.org/0009-0009-3671-1633>

Zhiyong Zeng  <https://orcid.org/0009-0006-3913-6337>

References

1. Kroesen M, Mulder HT, Van Holthe JML, et al. Confirmation of thermal dose as a predictor of local control in cervical carcinoma patients treated with state-of-the-art radiation therapy and hyperthermia. *Radiother Oncol.* 2019;140:150–158. doi:10.1016/j.radonc.2019.06.021
2. Dou Y, Kawaler EA, Cui Zhou D, et al. Proteogenomic characterization of endometrial carcinoma. *Cell.* 2020;180(4):729–748.e26. doi:10.1016/j.cell.2020.01.026
3. Varma KR, Dabbs DJ. Cervical carcinoma with divergent neuroendocrine and gastrointestinal differentiation. *Int J Gynecol Pathol.* 2018; 37(5):488–491. doi:10.1097/PGP.0000000000000438
4. Concin N, Matias-Guiu X, Vergote I, et al. ESGO/ESTRO/ESP guidelines for the management of patients with endometrial carcinoma. *Int J Gynecol Cancer.* 2021;31(1):12–39. doi:10.1136/ijgc-2020-002230
5. Wang Z, Wang J, Fan J, et al. Risk factors for cervical intraepithelial neoplasia and cervical cancer in Chinese women: Large study in Jiexiu, Shanxi province, China. *J Cancer.* 2017;8(6):924–932. doi:10.7150/jca.17416
6. Brüggmann D, Ouassou K, Klingelhöfer D, Bohlmann MK, Jaque J, Groneberg DA. Endometrial cancer: Mapping the global landscape of research. *J Transl Med.* 2020;18(1):386. doi:10.1186/s12967-020-02554-y
7. Taylan E, Oktay K. Fertility preservation in gynecologic cancers. *Gynecol Oncol.* 2019;155(3):522–529. doi:10.1016/j.ygyno.2019.09.012
8. Cheng H, Wang W, Zhang Y, et al. Expression levels and clinical significance of hepsin and HMGB1 proteins in cervical carcinoma. *Oncol Lett.* 2017;14(1):159–164. doi:10.3892/ol.2017.6116
9. Papathelemis T, Scharl S, Kronberger K, et al. Survival benefit of pelvic and paraaortic lymphadenectomy in high-grade endometrial carcinoma: A retrospective population-based cohort analysis. *J Cancer Res Clin Oncol.* 2017;143(12):2555–2562. doi:10.1007/s00432-017-2508-1
10. Plotti F, Terranova C, Luvero D, et al. Diet and chemotherapy: The effects of fasting and ketogenic diet on cancer treatment. *Chemotherapy.* 2020;65(3–4):77–84. doi:10.1159/000510839

11. Mauricio D, Zeybek B, Tymon-Rosario J, Harold J, Santin AD. Immunotherapy in cervical cancer. *Curr Oncol Rep*. 2021;23(6):61. doi:10.1007/s11912-021-01052-8
12. El-Sharkawy M, El-Mazny A, Ramadan W, et al. Three-dimensional ultrasonography and power Doppler for discrimination between benign and malignant endometrium in premenopausal women with abnormal uterine bleeding. *BMC Womens Health*. 2016;16(1):18. doi:10.1186/s12905-016-0297-3
13. Zhou J, Xiong Y, Ren Y, Zhang Y, Li X, Yan Y. Three-dimensional power Doppler ultrasonography indicates that increased placental blood perfusion during the third trimester is associated with the risk of macrosomia at birth. *J Clin Ultrasound*. 2021;49(1):12–19. doi:10.1002/jcu.22912
14. Schiffer VMMM, Pellaers D, Hoenen LJLM, Van Kuijk SMJ, Spaanderma MEA, Al-Nasiry S. Feasibility of three dimensional power Doppler ultrasonography methods to assess placental perfusion. *Eur J Obstet Gynecol Reprod Biol*. 2020;254:321–328. doi:10.1016/j.ejogrb.2020.08.006
15. Yang T, Tian S, Li Y, et al. Magnetic resonance imaging (MRI) and three-dimensional transvaginal ultrasonography scanning for pre-operative assessment of high risk in women with endometrial cancer. *Med Sci Monit*. 2019;25:2024–2031. doi:10.12659/MSM.915276
16. Zhang Y, Chen J, Zhen Z, Xu XY. Antidiastole value of three-dimensional ultrasonography and power Doppler between uterine parenchyma lumps and endometrial cancer: A retrospective study. *Curr Med Sci*. 2019;39(5):816–819. doi:10.1007/s11596-019-2110-7
17. Pandey H, Guruvare S, Kadavigere R, Rao CR. Utility of three dimensional (3-D) ultrasound and power Doppler in identification of high risk endometrial cancer at a tertiary care hospital in southern India: A preliminary study. *Taiwan J Obstet Gynecol*. 2018;57(4):522–527. doi:10.1016/j.tjog.2018.06.007
18. Zhang T, Qi J, Zhang C. The effect of three-dimensional ultrasound and magnetic resonance imaging in the staging diagnosis of endometrial cancer with hepatitis B virus infection and construction of mathematical model. *Results Phys*. 2021;25:104307. doi:10.1016/j.rinp.2021.104307
19. Liu SY, Ahsan Bilal M, Zhu JH, Li SM. Diagnostic value of serum human epididymis protein 4 in esophageal squamous cell carcinoma. *World J Gastrointest Oncol*. 2020;12(10):1167–1176. doi:10.4251/wjgo.v12.i10.1167
20. Lin D, Zhao L, Zhu Y, et al. Combination IETA ultrasonographic characteristics simple scoring method with tumor biomarkers effectively improves the differentiation ability of benign and malignant lesions in endometrium and uterine cavity. *Front Oncol*. 2021;11:605847. doi:10.3389/fonc.2021.605847
21. Li X, Cheng Y, Dong Y, et al. An elevated preoperative serum calcium level is a significant predictor for positive peritoneal cytology in endometrial carcinoma. *Chin J Cancer Res*. 2019;31(6):965–973. doi:10.21147/j.issn.1000-9604.2019.06.12
22. Asadollahi S, Mazaheri MN, Karimi-Zarchi M, Fesahat F, Farzaneh M. The relationship of *FOXR2* gene expression profile with epithelial-mesenchymal transition related markers in epithelial ovarian cancer. *Klin Onkol*. 2020;33(3):201–207. PMID:32683876.
23. Li B, Huang W, Cao N, Lou G. Forkhead-box R2 promotes metastasis and growth by stimulating angiogenesis and activating hedgehog signaling pathway in ovarian cancer. *J Cell Biochem*. 2018;119(9):7780–7789. doi:10.1002/jcb.27148
24. Lu SQ, Qiu Y, Dai WJ, Zhang XY. *FOXR2* promotes the proliferation, invasion, and epithelial-mesenchymal transition in human colorectal cancer cells. *Oncol Res*. 2017;25(5):681–689. doi:10.3727/096504016X14771034190471
25. Wang XH, Cui YX, Wang ZM, Liu J. Down-regulation of *FOXR2* inhibits non-small cell lung cancer cell proliferation and invasion through the Wnt/ β -catenin signaling pathway. *Biochem Biophys Res Commun*. 2018;500(2):229–235. doi:10.1016/j.bbrc.2018.04.046
26. Liao C, Zheng C, Wang L. Down-regulation of *FOXR2* inhibits hypoxia-driven ROS-induced migration and invasion of thyroid cancer cells via regulation of the hedgehog pathway. *Clin Exp Pharmacol Physiol*. 2020;47(6):1076–1082. doi:10.1111/1440-1681.13286
27. FIGO Committee on Gynecologic Oncology. FIGO staging for carcinoma of the vulva, cervix, and corpus uteri. *Int J Gynaecol Obstet*. 2014;125(2):97–98. doi:10.1016/j.ijgo.2014.02.003
28. Wei X, Su J, Yang K, et al. Elevations of serum cancer biomarkers correlate with severity of COVID-19. *J Med Virol*. 2020;92(10):2036–2041. doi:10.1002/jmv.25957
29. Ueno Y, Forghani B, Forghani R, et al. Endometrial carcinoma: MR imaging-based texture model for preoperative risk stratification. A preliminary analysis. *Radiology*. 2017;284(3):748–757. doi:10.1148/radiol.2017161950
30. Devine C, Gardner C, Sagebiel T, Bhosale P. Magnetic resonance imaging in the diagnosis, staging, and surveillance of cervical carcinoma. *Semin Ultrasound CT MRI*. 2015;36(4):361–368. doi:10.1053/j.sult.2015.05.004
31. Koh WJ, Abu-Rustum NR, Bean S, et al. Cervical Cancer, Version 3. 2019, NCCN Clinical Practice Guidelines in Oncology. *J Natl Compr Canc Netw*. 2019;17(1):64–84. doi:10.6004/jnccn.2019.0001
32. Harsh KK, Kapoor A, Paramanandhan M, et al. Induction chemotherapy followed by concurrent chemoradiation in the management of different stages of cervical carcinoma: 5-year retrospective study. *J Obstet Gynecol India*. 2016;66(5):372–378. doi:10.1007/s13224-015-0699-4
33. Matei D, Filiaci V, Randall ME, et al. Adjuvant chemotherapy plus radiation for locally advanced endometrial cancer. *N Engl J Med*. 2019;380(24):2317–2326. doi:10.1056/NEJMoa1813181
34. Banerjee S, Moore KN, Colombo N, et al. Maintenance olaparib for patients with newly diagnosed advanced ovarian cancer and a BRCA mutation (SOLO1/GOG 3004): 5-year follow-up of a randomised, double-blind, placebo-controlled, phase 3 trial. *Lancet Oncol*. 2021;22(12):1721–1731. doi:10.1016/S1470-2045(21)00531-3
35. Wang X, He B, Gao Y, Li Y. *FOXR2* contributes to cell proliferation and malignancy in human hepatocellular carcinoma. *Tumor Biol*. 2016;37(8):10459–10467. doi:10.1007/s13277-016-4923-3
36. Tian X, Zhang L, Jiao Y, Chen J, Shan Y, Yang W. CircABC10 promotes nonsmall cell lung cancer cell proliferation and migration by regulating the miR-1252/*FOXR2* axis. *J Cell Biochem*. 2019;120(3):3765–3772. doi:10.1002/jcb.27657
37. Xu W, Chang J, Liu G, Du X, Li X. Knockdown of *FOXR2* suppresses the tumorigenesis, growth and metastasis of prostate cancer. *Biomed Pharmacother*. 2017;87:471–475. doi:10.1016/j.biopha.2016.12.120
38. Song H, He W, Huang X, Zhang H, Huang T. High expression of *FOXR2* in breast cancer correlates with poor prognosis. *Tumor Biol*. 2016;37(5):5991–5997. doi:10.1007/s13277-015-4437-4
39. Deng X, Hou C, Liang Z, Wang H, Zhu L, Xu H. miR-202 suppresses cell proliferation by targeting *FOXR2* in endometrial adenocarcinoma. *Dis Markers*. 2017;2017:2827435. doi:10.1155/2017/2827435
40. Zhang S, Cheng J, Quan C, et al. circCELSR1 (hsa_circ_0063809) contributes to paclitaxel resistance of ovarian cancer cells by regulating *FOXR2* expression via miR-1252. *Mol Ther Nucleic Acids*. 2020;19:718–730. doi:10.1016/j.omtn.2019.12.005
41. Huang B, Sollee J, Luo YH, et al. Prediction of lung malignancy progression and survival with machine learning based on pre-treatment FDG-PET/CT. *EBioMedicine*. 2022;82:104127. doi:10.1016/j.ebiom.2022.104127
42. Suzuki S, Toyoma S, Abe T, et al. 18F-FDG-PET/CT can be used to predict distant metastasis in hypopharyngeal squamous cell carcinoma. *J Otolaryngol Head Neck Surg*. 2022;51(1):13. doi:10.1186/s40463-022-00568-8
43. Payday K, Seraj SM, Zadeh MZ, et al. The evolving role of FDG-PET/CT in the diagnosis, staging, and treatment of breast cancer. *Mol Imaging Biol*. 2019;21(1):1–10. doi:10.1007/s11307-018-1181-3
44. Albano D, Zizioli V, Odicino F, Giubbini R, Bertagna F. Clinical and prognostic value of 18F-FDG PET/CT in recurrent endometrial carcinoma [in Spanish]. *Rev Esp Med Nucl Imagen Mol (Engl Ed)*. 2019;38(2):87–93. doi:10.1016/j.remn.2018.09.005
45. Lawal IO, Ololade KO, Popoola GO, et al. 18F-FDG-PET/CT imaging of uterine cervical cancer recurrence in women with and without HIV infection. *Q J Nucl Med Mol Imaging*. 2022;66(1):52–60. doi:10.23736/S1824-4785.19.03156-X
46. Unal D, Sedelaar JPM, Aarnink RG, et al. Three-dimensional contrast-enhanced power Doppler ultrasonography and conventional examination methods: The value of diagnostic predictors of prostate cancer. *BJU Int*. 2007;86(1):58–64. doi:10.1046/j.1464-410x.2000.00719.x
47. Huang YF, Cheng YM, Wu YP, et al. Three-dimensional power Doppler ultrasound in cervical carcinoma: Monitoring treatment response to radiotherapy. *Ultrasound Obstet Gynecol*. 2013;42(1):84–92. doi:10.1002/uog.11223

48. Xu Y, Zhu L, Ru T, et al. Three-dimensional power Doppler ultrasound in the early assessment of response to concurrent chemo-radiotherapy for advanced cervical cancer. *Acta Radiol.* 2017;58(9):1147–1154. doi:10.1177/0284185116684677
49. Belitsos P, Papoutsis D, Rodolakis A, Mesogitis S, Antsaklis A. Three-dimensional power Doppler ultrasound for the study of cervical cancer and precancerous lesions. *Ultrasound Obstet Gynecol.* 2012;40(5): 576–581. doi:10.1002/uog.11134
50. Alcázar JL. Tumor angiogenesis assessed by three-dimensional power Doppler ultrasound in early, advanced and metastatic ovarian cancer: A preliminary study. *Ultrasound Obstet Gynecol.* 2006;28(3): 325–329. doi:10.1002/uog.3804
51. Li KT, Jiang ZH, Tian JW, Liu YJ, Ren M. The value of Mainz ultrasound scoring system combined with 3D-power Doppler ultrasound in differentiating benign and malignant pelvic masses. *Chin J Ultrasonography.* 2018;1:53–57. <https://rs.yiigle.com/cmaid/1028613>. Accessed April 1, 2023.
52. Fu S, Niu Y, Zhang X, Zhang JR, Liu ZP, Wang RT. Squamous cell carcinoma antigen, platelet distribution width, and prealbumin collectively as a marker of squamous cell cervical carcinoma. *Cancer Biomark.* 2018;21(2):317–321. doi:10.3233/CBM-170442
53. Chmura A, Wojcieszek A, Mrochem J, et al. Usefulness of the SCC, CEA, CYFRA 21.1, and CRP markers for the diagnosis and monitoring of cervical squamous cell carcinoma [in Polish]. *Ginekol Pol.* 2009;80(5): 361–366. https://journals.viamedica.pl/ginekologia_polska/article/download/46612/33399. Accessed April 10, 2009.
54. Tsai CC, Liu YS, Huang EY, et al. Value of preoperative serum CA125 in early-stage adenocarcinoma of the uterine cervix without pelvic lymph node metastasis. *Gynecol Oncol.* 2006;100(3):591–595. doi:10.1016/j.ygyno.2005.09.049